Ceramics International 43 (2017) 9831–9837

Contents lists available at ScienceDirect

Ceramics International

journal homepage: www.elsevier.com/locate/ceramint

# Microstructural differences between electrospun alumina borate nanofibers prepared by solutions with different PVP contents

Xiaolei Song, Wensheng Liu, Juan Wang, Shuheng Xu, Bing Liu, Jijin Liu, Yunzhu Ma*

*State Key Laboratory of Powder Metallurgy, Central South University, Changsha 410083, China*

ARTICLE INFO

*Keywords:*
Alumina borate
Nanofibers
Electrospinning
Microstructure
Polyvinyl pyrrolidone

ABSTRACT

Alumina borate nanofibers were fabricated by electrospinning combined with sol-gel method using aluminum acetate ($Al(OH)_2(OOCCH_3)\cdot 1/3H_3BO_3$, stabilized with boric acid) and polyvinyl pyrrolidone (PVP) as raw materials. As-spun composite nanofibers were electrospun from the spinning solutions prepared with different PVP contents. The as-spun nanofibers were calcined at 1000 °C and the microstructures of the calcined nanofibers were investigated. The results showed that with the content of PVP increased, the diameters of the alumina borate nanofibers increased, and the temperatures at which the $Al_4B_2O_9$ phase formed and $Al_4B_2O_9$ transformed to $Al_{18}B_4O_{33}$ also increased. However, the crystallinity of the calcined nanofibers decreased with the increase of the PVP content. The grains became smaller and more uniform due to the increasing amount of voids and cracks generated by the decomposition of PVP.

## 1. Introduction

Alumina borate materials in $Al_2O_3$-$B_2O_3$ binary system are attractive ceramic materials with excellent mechanical properties, high melting point, low thermal expansion, low density and good chemical inertness [1,2]. In recent years, one-dimensional (1D) micro-/nano-scale materials have become the focus of a significant research effort due to their novel properties, unique structure and potential applications in many areas [3]. A variety of advanced techniques have been used to prepare 1D micro-/nano-scale materials with desired chemical composition and morphology. Consequently, alumina borate materials with 1D micro-/nano-structure, such as whiskers, nanorods, nanowires and nanotubes, have been fabricated [4–8]. They are widely used as reinforcement for metal matrix composites (MMCs), heating-insulating materials, and filter media, etc [2,9]. The conventional methods to prepare these products include chemical vapor deposition, molten salt method, catalytic synthesis, high-temperature solid-state reaction, low-heating-temperature solid-state precursor method, direct calcinations of a precursor, flux method and sol-gel method [6,8,10,11]. However, disadvantages can hardly be avoided for most of the mentioned methods, including high energy consumption, inevitable formation of by-products which leads to the low yield of the products, and additionally, the multistep process are more complicated to control. Furthermore, the relatively small aspect ratio of the alumina borate nanorods, nanowires, or nanowhiskers also limits their potential applications.

Dai et al. [12] were the first to prepare alumina borate fibers in nano-scale successfully. Compared with the nano-scale products mentioned above, such fibers were continuous with more uniform diameters and larger aspect ratio, which might significantly expand their applications. In their study, electrospinning was adopted to synthesize the fibers. This technique is superior to the preparation method mentioned above because it is relatively less complicated to process, easily-controlled and high-yielding. It has been regarded as the most versatile method to prepare nanofibers made of various materials in the past decades [13,14]. When preparing ceramic nanofibers, electrospinning is normally combined with the sol-gel method. The spinning solution is obtained by mixing the precursor sol and the dissolved polymer. The polymers serve as the carriers of precursor gels in transforming the spinning solution to fiber-like structure. Ozdemir et al. [15] synthesized alumina borate nanofibers using PVA with different concentrations. It was found that nanofibers with larger diameter were obtained when the content of PVA contained in the spinning solution increased. Researchers within this area also reported that the morphology of the ceramic nanofibers could be influenced by the polymers addition in the spinning solution [16,17]. Thus, for the purpose of preparing nanofibers with desired diameters, controlling the proportions of polymers in spinning solutions is an effective way.

The growth of the grains during crystallization can hardly be ignored for alumina borate nanofibers. Particularly, the crystallization behavior of the alumina borate nanofibers is associated with their structure stability under high-temperature environment. Dai et al. [12]

* Corresponding author.
*E-mail address:* zhuzipm@csu.edu.cn (Y. Ma).

http://dx.doi.org/10.1016/j.ceramint.2017.04.163
Received 26 November 2016; Received in revised form 23 April 2017; Accepted 27 April 2017
Available online 28 April 2017

also studied the crystalline phase of the ultra-fine alumina borate fibers calcined at different temperatures. It was found that the $Al_4B_2O_9$ phase formed at 1000 ℃, with slight concentration of the $Al_{18}B_4O_{33}$ phase. Grains can be easily observed with large quantity on the coarse surface of the fibers. When calcination temperature increased to 1200 ℃, increasing amount of $Al_{18}B_4O_{33}$ phase formed and the grain sizes increased significantly. They also pointed out that the PVA they selected as the polymer additive decomposed during calcination, which is consistent with other studies regarding the removal of polymers while preparing ceramic nanofibers by electrospinning [18,19]. Although the decomposition of the polymers during calcining was observed, very little information has been reported about the influence of the use of polymers or the content of polymers in as-spun fibers on the crystallization behavior and grain growth of the alumina borate nanofibers, as well as other ceramic oxide nanofibers after heating.

In the current work, alumina borate nanofibers were fabricated using aluminum acetate stabilized with boric acid and polyvinyl pyrrolidone (PVP) as raw materials. The spinning solutions were prepared with different mass ratio of PVP solution to precursor sol. The as-spun composite nanofibers were calcined at 1000 ℃ to obtain the final fiber products. The morphology, crystallization temperatures and grain sizes of the alumina borate nanofibers were investigated. The mechanism of which the voids and cracks influence on grain sizes of the ceramic nanofibers was also discussed.

## 2. Experimental procedure

Aluminum acetate ($Al(OH)_2(OOCCH_3)\cdot 1/3H_3BO_3$, stabilized with boric acid) was supplied by Strem Chemicals, Inc.. PVP with a molecular weight of 1,300,000 was supplied by Tianjin Bodi Chemical Co., Ltd.. Ethanol was offered by Tianjin Hengxing Chemical Reagent Co., Ltd.. Deionized water was prepared in the laboratory.

1 g aluminum acetate was added into 4 g solvent (2 g deionized water mixed with 2 g alcohol) and stirred at 40 ℃ for 12 h to prepare precursor sol. Part of the precursor sol was dried at 60 ℃ to form precursor gel and then was grounded to powders for comparative studies. PVP solution with a concentration of 16 wt% was prepared using alcohol as the solvent. To prepare homogeneous spinning solutions with different PVP contents, pre-prepared PVP solution and precursor sol were mixed with different mass ratio and stirred for 1 h at room temperature. The mass ratio of PVP solution to precursor sol, as well as the conductivity and viscosity, of the spinning solutions were detailed in Table 1.

The spinning solutions were transferred into a plastic syringe equipped with a metallic needle, which was connected to a negative voltage supply. Electrospinning was operated at the voltage of −6 kV. The feeding rate controlled by a syringe pump was kept at 0.45 ml/h and the distance between the needle tip and the collector was 15 cm. The as-spun composite nanofibers were dried by an oven to remove the residual solvent. Then the fibers were heated to 1000 ℃ with a heating rate of 5 ℃/min and kept at 1000 ℃ for 1 h to obtain alumina borate nanofibers.

The conductivity and viscosity of the spinning solutions were measured by a digital conductivity meter (DDS-11A, Leici, China) and a digital viscometer (SNB-1A, Fangrui, China) at 25 ℃, respectively. The average value of each parameter was calculated after five measurements for each sample. The morphology of the as-spun composite nanofibers and alumina borate nanofibers was examined by scanning electron microscopy (SEM, Helios NanoLab G3 UC, FEI, Czech). The diameters of the fibers were calculated using the image analysis software Image J. Thermogravity-differential scanning calorimeter (TG-DSC) analysis of as-spun composite nanofibers was performed on a thermoanalyzer (STA449C, Netzsch, German) in air atmosphere at a heating rate of 10 ℃/min. The X-ray powder diffraction (XRD) data of calcined samples were obtained by a diffractometer (D/max2500 PC, Rigaku, Japan) with CuKα radiation in the region of $5 < 2\theta < 80°$. Additionally, transmission electron microscope (TEM, JEM-2100F, JEOL, Japan) was also employed to observe the distribution of the crystal grains in the alumina borate nanofibers.

**Table 1**
The mass ratio of PVP solution to precursor sol, conductivity and viscosity of the spinning solutions.

| Sample No. | Mass ratio of PVP solution to precursor sol | Conductivity (μS/cm) | Viscosity (mPa s) |
|---|---|---|---|
| 1# | 0.6 | 297 | 577 |
| 2# | 1.28 | 204 | 692 |
| 3# | 3.0 | 141 | 989 |

## 3. Results and discussion

### 3.1. Fiber morphology

Fig. 1 shows the SEM images and diameter distribution histograms of the as-spun composite nanofibers. As can be observed, continuous fibers with smooth surface and cylindrical morphology were obtained by electrospinning the spinning solutions with different mass ratio of PVP solution to precursor sol. When the ratio was 0.6, the average diameter of the nanofibers was about 404 nm. When the ratio increased to 1.28, the average diameter reached up to 813 nm and when the ratio went up to 3, the diameter was 1154 nm. As illustrated in Table 1, the viscosity of the spinning solution increased along with the mass ratio, and the conductivity of the spinning solution showed the contrary tendency. Consequently, the as-spun fibers had larger diameters. Since alcohol and water were almostly removed during electrospinning and drying process, it could be concluded that the as-spun fibers which generated from spinning solutions containing larger amount of PVP solution also had larger PVP content.

Fig. 2 exhibits the SEM images and diameter distribution histograms of alumina borate nanofibers calcined at 1000 ℃. As displayed in Fig. 2, the continuous and cylindrical morphology of the nanofibers was kept after the calcination process. Such phenomenon revealed that PVP was a good structure-directing polymer additive. High magnification SEM images showed that the surface of the calcined nanofibers was covered with large number of tiny particles, and the dimension of such particles increased when PVP content increased. However, it was unable to ensure from SEM measurement individually that the particles were caused by the grain growth, or the rapid removal of decomposed products in the present work. In addition, voids and cracks were also observed on the fiber surface, and they increased in size and number with PVP content increased as well. Obviously, this was ascribed to the escape of the increasing amount of the decomposition products resulted from higher content of PVP in the as-spun fibers. The average diameters of the alumina borate nanofibers decreased to 287 nm, 397 nm and 481 nm, respectively. The reduction in diameters of the nanofibers was ascribed to the removal of PVP and other organics. According to the investigation, the larger shrinkages in diameters of the calcined nanofibers were associated with the increased contents of PVP in as-spun composite nanofibers.

### 3.2. Heating process

TG curves of the precursor gel, as-spun composite nanofibers with different PVP contents, as well as pure PVP fibers are shown in Fig. 3. For alumina gel (Fig. 3(a)), weight loss could hardly be observed after 630 ℃, indicating that the decomposition products of boric acid and organic groups had been removed entirely. Fig. 3(e) showed that the weight residue of the pure PVP fibers became zero at 675 ℃, which revealed that PVP decomposed completely at that temperature.

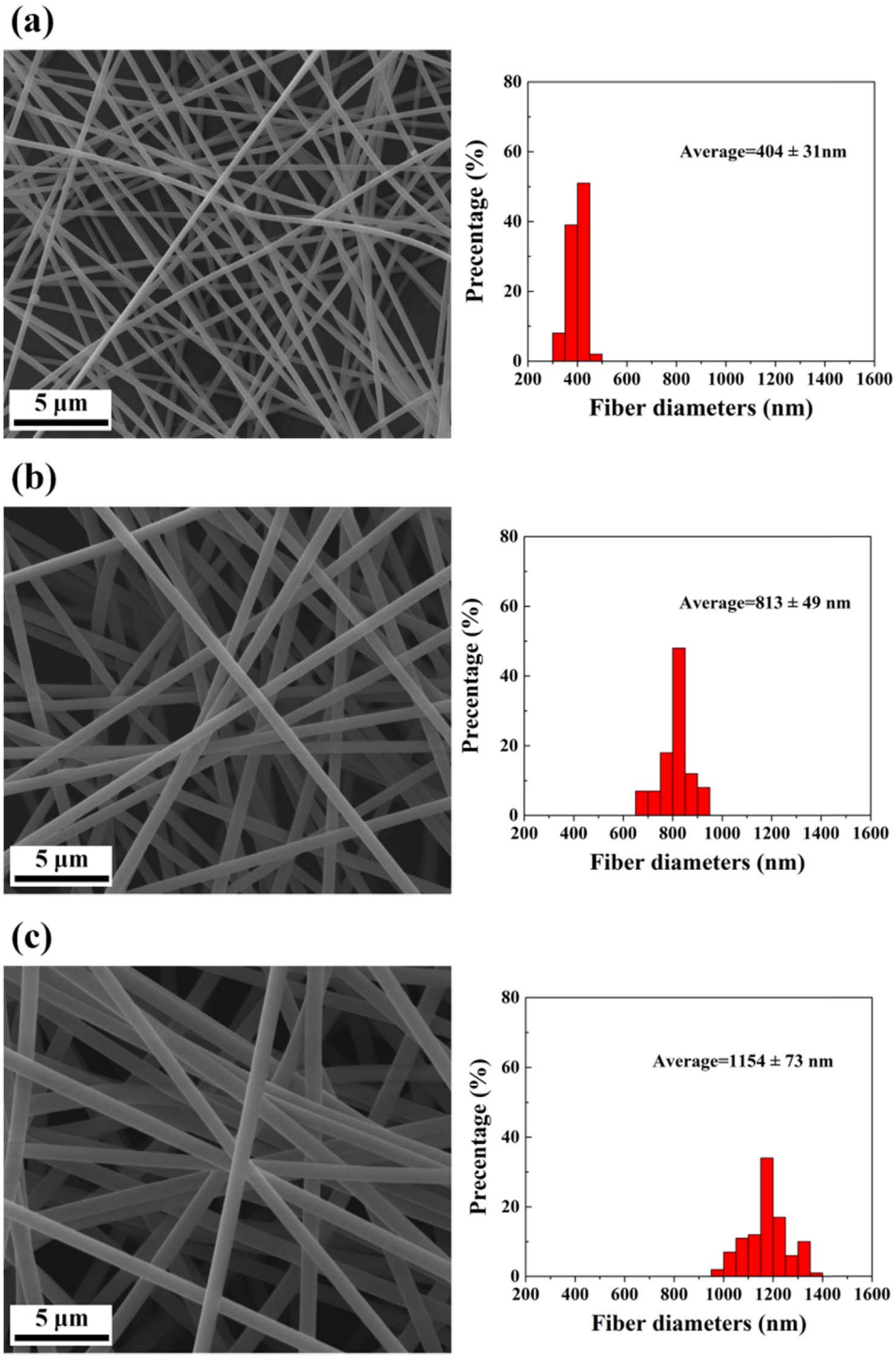


**Fig. 1.** SEM images and diameter distribution histograms of as-spun composite nanofibers prepared from (a) sample 1#, (b) sample 2# and (c) sample 3#.

However, to the as-spun composite nanofibers shown in curves (b), (c) and (d), the temperatures that the residue weight started to remain unchanged were approximately 740 ℃, 770 ℃ and 805 ℃, respectively. It can be deduced that the precursor gel and PVP in as-spun composite nanofibers slowed down the decomposition rate of each other during heat-treatment process. In addition, the as-spun nanofibers with larger diameters had smaller surface areas, which would weaken the heat and mass transfer process and reduce the reaction interface of decomposition. So the decomposition rate of PVP and other organics, as well as the removal rate of the decomposition products, would be decreased while heating. This may explain the feature of the TG curves. Therefore, a proper PVP content is necessary for an efficient calcination when fabricating alumina borate nanofibers by electrospinning.

Fig. 4 shows the DSC curves of precursor gel and as-spun composite nanofibers with different PVP contents. Only one exothermic peak was evident for the precursor gel but two exothermic peaks could be observed for the as-spun nanofibers. The exothermic peak at 891 ℃ for precursor gel showed in Fig. 4(a) was associated with the onset of crystallization of the $Al_4B_2O_9$ phase [20]. However, the corresponding exothermic peaks of the as-spun nanofibers appeared at 897 ℃, 912 ℃

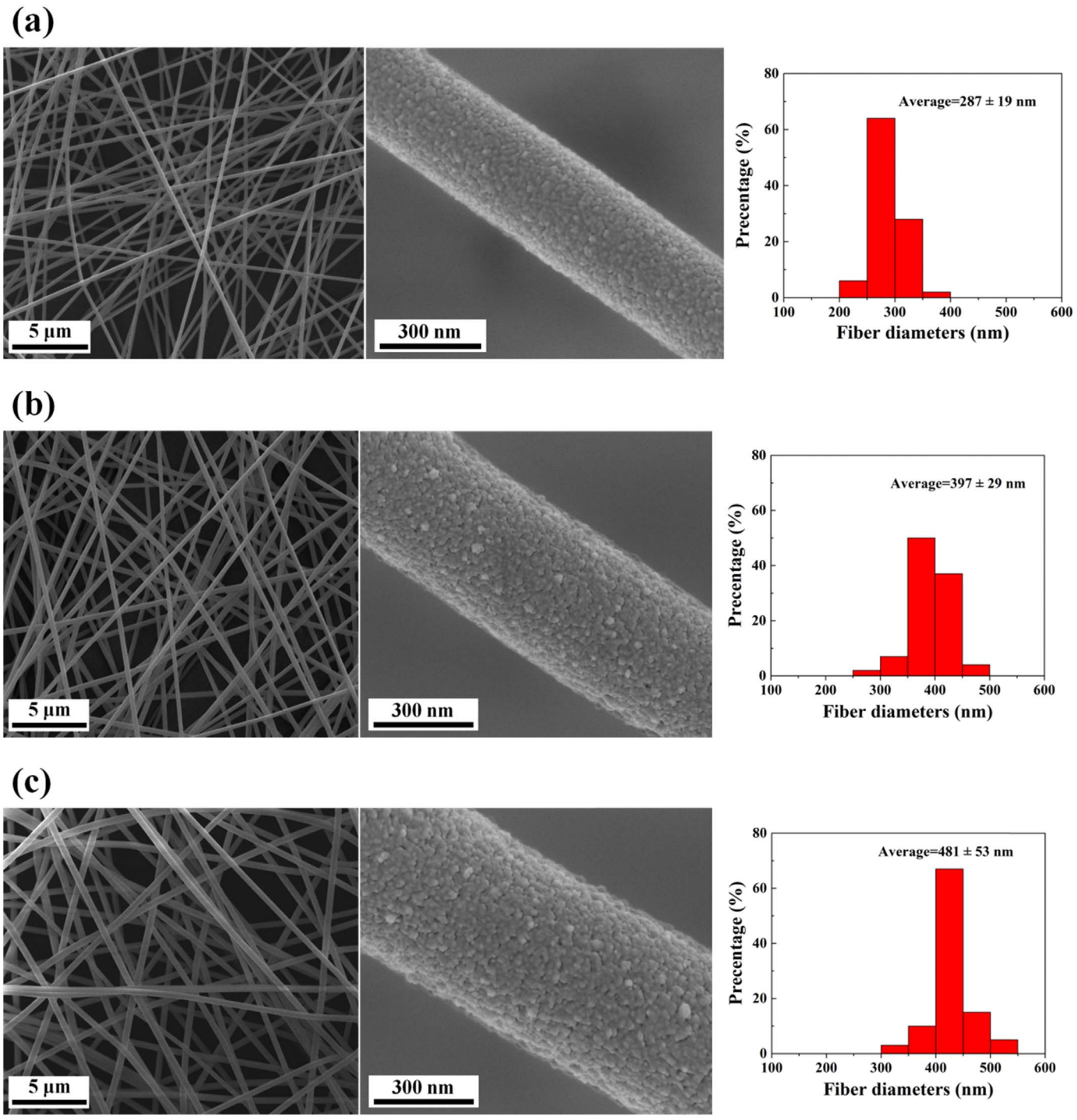


**Fig. 2.** SEM images at various magnifications and diameter distribution histograms of alumina borate nanofibers prepared from (a) sample 1#, (b) sample 2# and (c) sample 3# after calcining at 1000 ℃.

and 921 ℃ respectively, which indicated that the temperatures of crystallization increased. The broad exothermic peaks at 1095 ℃, 1120 ℃ and 1131 ℃ as seen in Fig. 4(b), (c) and (d) were attributed to the phase transition from $Al_4B_2O_9$ to $Al_{18}B_4O_{33}$ [20], revealing that the temperatures of phase transition rose as well with PVP content increased.

### 3.3. Grain size

Fig. 5 shows the XRD patterns of alumina borate powders and alumina borate nanofibers calcined at 1000 ℃. For all samples, phase transformation to $Al_4B_2O_9$ can be observed, while the $Al_{18}B_4O_{33}$ phase cannot be detected. This was consistent with the conclusion given from the DSC curves. However, the intensities of the characteristic peaks of the calcined samples were different. As observed, lower intensities were evident along with the increased PVP contents. Since no other phase generated in the current situation, the weaker diffraction peaks indicated that the crystallinity of $Al_4B_2O_9$ was lower.

The data from XRD patterns were used to calculate the crystallite sizes of the alumina borate powders and nanofibers by Scherrer equation as followed:

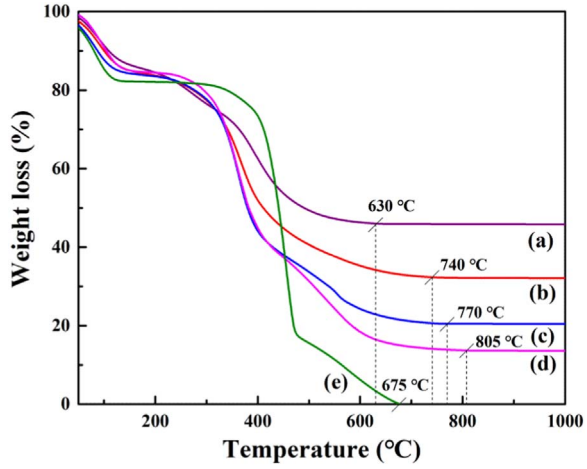


**Fig. 3.** TG curves of (a) precursor gel, as-spun composite nanofibers prepared from (b) sample 1#, (c) sample 2# and (d) sample 3#, and (e) pure PVP fibers.

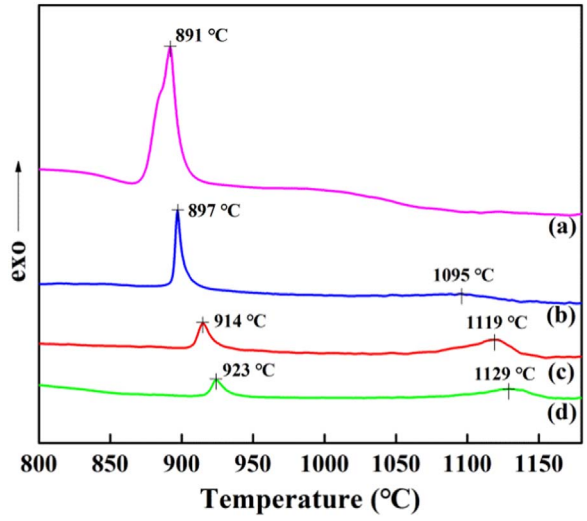


**Fig. 4.** DSC curves of (a) precursor gel and as-spun composite nanofibers prepared from (b) sample 1#, (c) sample 2# and (d) sample 3#.

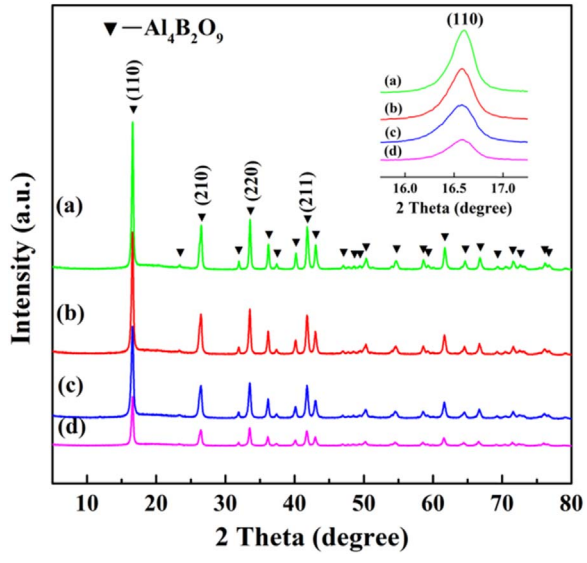


**Fig. 5.** XRD patterns of (a) alumina borate powders and alumina borate nanofibers prepared from (b) sample 1#, (c) sample 2# and (d) sample 3# after calcining at 1000 °C.

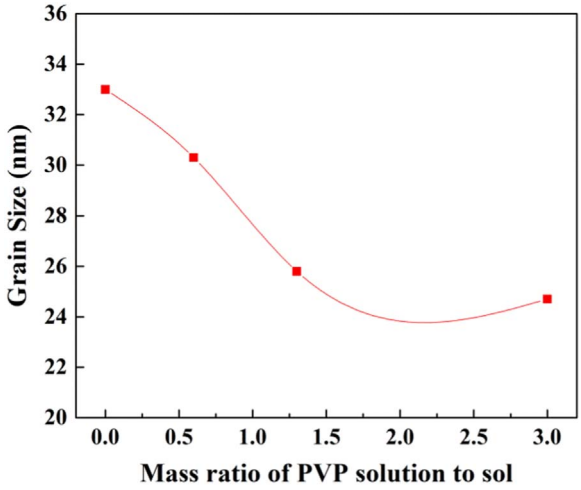


**Fig. 6.** Crystallite sizes of alumina borate powders and alumina borate nanofibers obtained from sample 1#–3#.

$$s = \frac{K\lambda}{\beta_{1/2}\cos\theta}$$

where $s$ is the crystallite size (Å), $\lambda$ is the wave length of the incident radiations, $\beta_{1/2}$ is the FWHM of the Bragg peak, $\theta$ is the Bragg angle of diffraction peaks that selected to calculate the crystallite size and $K$ is the Scherrer constant. The $K$ value varies between 0.9 and 1.2 depending on the shape of the particle (e.g. spherical, cubic or otherwise). In the present work, we used a value of 0.94 for $K$ for the most intense diffraction peak of (110) planes that displayed in the insert in Fig. 5. The crystallite sizes of the calcined samples are shown in Fig. 6. The alumina borate powders had an average crystallite size of 33.0 nm. While for the calcined nanofibers prepared from solutions with increased amount of dissolved PVP, the crystallite sizes reduced from 30.3 nm to 24.7 nm.

The crystallite sizes obtained by the calculation based on the XRD results could also be verified from the TEM images of the ceramic nanofibers shown in Fig. 7. The calcined nanofibers prepared from spinning solution sample 1# displayed in Fig. 7(a) were composed of many interconnected and nonuniform grains. While for the nanofibers obtained from sample 2# exhibited in Fig. 7(b), the grains became small and relatively uniform. And the grains in the nanofibers prepared from sample 3# were the smallest and most uniform as observed in Fig. 7(c). Besides, it could also be seen that the fibers obtained from the sample with lower PVP content showed worse crystallization behavior determined by the HRTEM images and the electronic diffraction (ED) patterns in Fig. 7.

Based on the analyses above, it could be concluded that the particles on the fiber surface observed from SEM images should not be considered as crystal grains and they were normally formed due to the rapid removal of decomposed gases. Therefore, the sizes of these particles were proportional to the PVP content in as-spun fibers.

### 3.4. Influencing mechanism

For alumina borate nanofibers, during the calcination process, tiny grains will grow up and the adjacent grains also tend to combine with each other to form larger grains. As discussed in Section 3.1, voids and cracks on the nanofibers increased in size and number when PVP content increased. This had significant effects on the grain sizes of the alumina borate nanofibers. The possible influencing mechanism is illustrated in Fig. 8. Fig. 8(a) displays the effect of these defects on the sizes of the grains for the fibers obtained from solutions with low content of PVP. At stage I, tiny primary grains generated first. While at

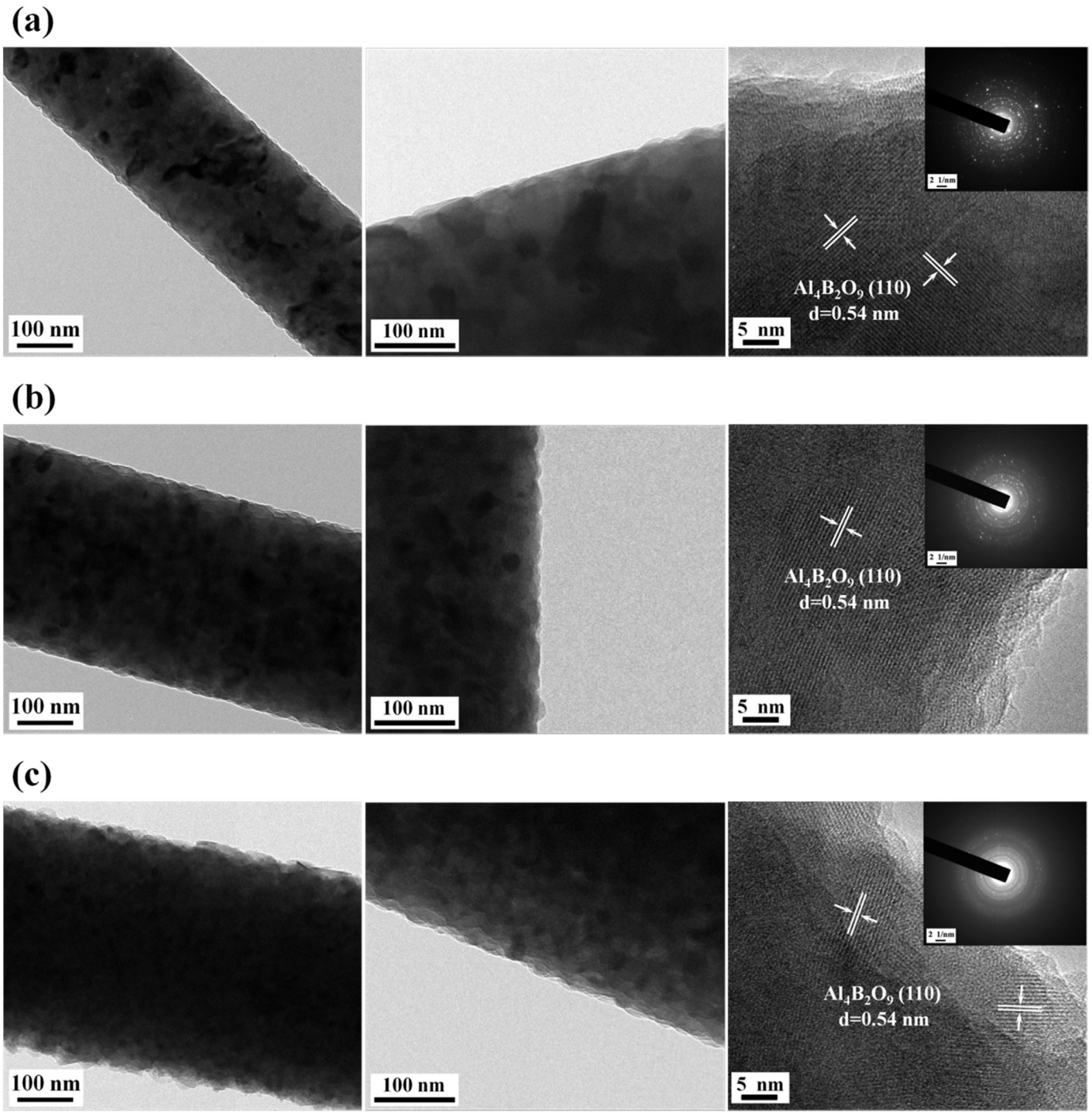


**Fig. 7.** TEM images of alumina borate nanofibers prepared from (a) sample 1#, (b) sample 2# and (c) sample 3# after calcining at 1000 ℃.

stage II, large fraction of tiny grains grew individually or merged with adjacent ones to form large $Al_4B_2O_9$ grains. This was because that less voids and cracks hindered the diffusion of the grain boundaries. Thus, large and nonuniform grains were formed. However, for the fibers produced by high content of PVP as displayed in Fig. 8(b), increased number of voids and cracks emerged at the positions between the tiny primary grains, which made the grain boundaries difficult to diffuse. Therefore, the grains were small and uniform.

## 4. Conclusions

Alumina borate nanofibers were fabricated by calcining the as-spun composite nanofibers electrospun from the spinning solutions with different mass ratio of PVP solution to precursor sol at 1000 ℃. The precursor sol was prepared using aluminum acetate stabilized with boron as raw materials. With the increase of PVP content in the spinning solution, the obtained alumina borate nanofibers became thicker and coarser, and the voids and cracks on fiber surface increased in size and number. In addition, the crystallization temperatures of $Al_4B_2O_9$ phase increased, the intensities of the characteristic peaks of $Al_4B_2O_9$ phase weakened, and the grain sizes became smaller and more uniform. The current work revealed that PVP content in spinning solution had significant influences on the microstructure of the alumina borate nanofibers, which might eventually affect their properties.

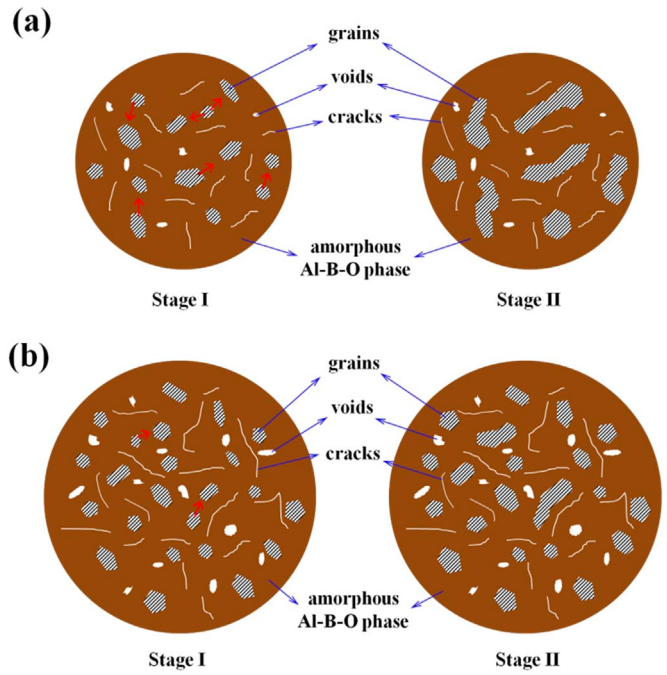


**Fig. 8.** Possible influencing mechanism of voids and cracks on grain sizes of alumina borate nanofibers prepared from solutions with (a) low content and (b) high content of PVP. Stage I and II show the generation of tiny primary grains and the merging and growth of tiny grains, respectively.

## Acknowledgements

The authors gratefully acknowledge the financial support from the "Chang Jiang Scholars Program" of the Ministry of Education of China (Grant no. T2011119).

## References

[1] J. Zhang, J. Lin, H.S. Song, E.M. Elssfah, S.J. Liu, J.J. Luo, et al., Bulk-quantity fast production of $Al_4B_2O_9/Al_{18}B_4O_{33}$ single-crystal nanorods by a novel technique, Mater. Lett. 60 (2006) 3292–3295.
[2] J. Wang, G. Ning, X. Yang, Z. Gan, H. Liu, Y. Lin, Large-scale synthesis of $Al_4B_2O_9/Al_{18}B_4O_{33}$ whiskers via a novel method, Mater. Lett. 62 (2008) 1208–1211.
[3] P.M. Rorvik, T. Grande, M.A. Einarsrud, One-dimensional nanostructures of ferroelectric perovskites, Adv. Mater. 23 (2011) 4007–4034.
[4] H. Wada, K. Sakane, H. Hata, S.C. Corporation, Synthesis of Aluminium Borate Whiskers in Potassium Sulphate Flux, 10, 1991, pp. 1076–1077.
[5] C.A. Min, Synthesis, Structure and Growth Mechanism of Aluminum Borate Nanorods, 25, 2009, pp. 2570–2574.
[6] I. Gonzalez-Martinez, A. Bachmatiuk, S. Gorantla, J. Kunstmann, V. Bezugly, T. Gemming, et al., Defect assisted thermal synthesis of crystalline aluminum borate nanowires, J. Appl. Phys. 112 (2012).
[7] E.M. Elssfah, C.C. Tang, J. Zhang, H.S. Song, X.X. Ding, S.R. Qi, Low-temperature performance of $Al_4B_2O_9$ nanowires, Mater. Res. Bull. 42 (2007) 482–486.
[8] Y. Li, R.P.H. Chang, Synthesis and characterization of aluminum borate ($Al_{18}B_4O_{33}$, $Al_4B_2O_9$) nanowires and nanotubes, Mater. Chem. Phys. 97 (2006) 23–30.
[9] R. Ma, Y. Bando, T. Sato, C. Tang, F. Xu, Single-crystal $Al_{18}B_4O_{33}$ microtubes, J. Am. Chem. Soc. 124 (2002) 10668–10669.
[10] S. Peng, H. Jinwen, W. Wenwei, W. Xuehang, Preparation of aluminum borate whiskers by the molten salt synthesis method, Ceram. Int. 39 (2013) 7263–7267.
[11] J. Zhou, D. Su, J. Luo, M. Zhong, Synthesis of aluminum borate nanorods by a low-heating-temperature solid-state precursor method, Mater. Res. Bull. 44 (2009) 224–226.
[12] H. Dai, J. Gong, H. Kim, D. Lee, A novel method for preparing ultra-fine alumina-borate oxide fibres via an electrospinning technique, Nanotechnology 13 (2002) 674.
[13] Y. Dzenis, Material science. Spinning continuous fibers for nanotechnology, Science 304 (2004) 1917–1919.
[14] M. Inagaki, Y. Yang, F. Kang, Carbon nanofibers prepared via electrospinning, Adv. Mater. 24 (2012) 2547–2566.
[15] M. Ozdemir, E. Celik, U. Cocen, Effect of viscosity on the production of alumina borate nanofibers via electrospinning, Mater. Tehnol. 47 (2013) 735–738.
[16] M. Mohammad Ali Zadeh, M. Keyanpour-Rad, T. Ebadzadeh, Synthesis of mullite nanofibres by electrospinning of solutions containing different proportions of polyvinyl butyral, Ceram. Int. 39 (2013) 9079–9084.
[17] N. Koji, S. Mikita, I. Satoshi, et al., Alumina nanofibers obtained from poly(vinyl alcohol)/boehmite nanocomposites, J. Appl. Polym. Sci. 121 (3) (2011) 1774–1779.
[18] J.H. Kim, S.J. Yoo, D.H. Kwak, H.J. Jung, T.Y. Kim, K.H. Park, et al., Characterization and application of electrospun alumina nanofibers, Nanoscale Res. Lett. 9 (2014) 44.
[19] A.F. Lotus, R.K. Feaver, L.A. Britton, E.T. Bender, D.A. Perhay, N. Stojilovic, et al., Characterization of $TiO_2$-$Al_2O_3$ composite fibers formed by electrospinning a sol-gel and polymer mixture, Mater. Sci. Eng. B Solid-State Mater. Adv. Technol. 167 (2010) 55–59.
[20] X. Tao, X. Wang, X. Li, Nanomechanical characterization of one-step combustion-synthesized $Al_4B_2O_9$ and $Al_{18}B_4O_{33}$ nanowires, Nano Lett. 7 (2007) 3172–3176.